

Meta-Heuristic Optimization Techniques for control of Hybrid Electrical Energy Sources

Swapnil Srivastava

Electrical Engineering Department
United College of Engineering and Research, Prayagraj, UP, India
swapnilsrivastava@united.ac.in

Sanjay Kumar Maurya (PhD)

Electrical Engineering Department
GLA University, Mathura, UP, India
sanjay.maurya@gla.ac.in

Abstract

Background: Hybrid Electric Vehicle (HEV) uses two sources of energy namely primary and auxiliary source. If only the battery bank is used as a power source of vehicle, then the performance of the vehicle is not satisfactory due to continuous charging and discharging mode, also the direction and amount of the battery current are changed continuously causing stress in the battery bank.

Objectives: Objective of the proposed work to control the power flow between battery and supercapacitor (SC) so as the dc bus voltage remains constant. The error is speed is to be minimised for desired operating conditions.

Methods: The objective is achieved by using the unidirectional buck-boost converter with battery bank and bidirectional buck-boost converter with SC Auxiliary source provides the energy during acceleration and store the energy at the time of braking. The controller with tuned PID parameters ensures the responses of quickly with minimal overshoot. This paper presents control technique for a Battery and Supercapacitor operated HEV and the tuning of PID controller using Teaching Learning Based Optimization (TLBO), particle swarm optimization (PSO), and Gray Wolf Optimization (GWO). The results are compared under various operating condition on the performance parameters integral absolute error (IAE), integral squared error (ISE), integral of the time-weighted absolute of the error (ITAE) and integral of the time-squared of the error (ITSE).

Conclusions: The result suggests the PID parameters tuned with GWO technique give minimum error coefficients, The error is further reduced when SC is introduced with the battery as input source.

Keywords: Battery, Supercapacitor, UBBC, BBBC, PSO, GWO, TLBO.

1. Introduction

The fossil fuels are the major contributors of world energy scenario [1]. The world very recently has witnessed an energy crisis in terms of shortage of coal supplies and other fossil fuel reserves impacting energy-intensive industries and bulk power-consuming factories[2].The situation is no better in the Indian subcontinent as well, with grid outages experienced in nearby countries in January 2021 [3] and Indian coal reserves dwindling for over a fortnight Sep-Oct 2021[4].The use of fossil fuels for power generation may further be curtailed by mandates and sanctions as speculated ahead of the UN Climate Change Conference (COP26), UK Nov 2021[5], Furthermore India has pledged to curtail greenhouse gases to net zero-till 2070 in the COP26 meet in Glasgow[6].

New solid-state battery technology has stepped in at the most opportune moment to fill in the void created by reduced fossil fuel usage. Solid-state batteries promise higher energy density, extended cycles, and faster charging which are quintessential for working in tandem with supercapacitors in onboard energy storage for use in EV/HEV/PHEV, Tramways, and other transport equipment.The best clean option for hybrid EVs is Fuel cell hybrid but technical/security constraints have till now kept them in beta phases. Peripheral Extended Component Interconnect architecture from National Instruments has been used in [7] to analyze power supply operation by matching it against vehicle load simulator. Comprehensive control for structural cost and performance optimization through a Genetic Algorithm could

be used for fuel cell-based powertrain as deterministic rule control may compromise security during speed manoeuvres [8].

Battery and supercapacitor cost analysis is effectively done by rainflow model which suggests analysis of SOC from the maximum value and then determining the discharge cycle from top to bottom. GA based optimization technique minimizes the cycling cost [9]. Energy regeneration during braking further reduces the daily operational cost. The degradation approach is used with hybrid ESS sizing [10]. Fuzzy logic controller (FLC) with adaptive PI charge controller is used for effective power distribution between battery and SC. The allocation of braking energy to SC reduces the power loss, stress and temperature of battery [11]. The split of power gives an opportunity for engine to run at its optimum operating point. The rule base is developed based on efficiency map of vehicle components [12]. SC voltage for efficiency and safety concern is also an important parameter. An λ - control based optimization method keeps the SC voltage in suitable limits [13]. Wavelet transform is utilized in determining high frequency components of current so as it can be distributed to SC [14]. Driving pattern recognition further decreases the maximum charge-discharge current thereby improving the battery life cycle [15]. The use of multi input converters regulates the SOC for SC and makes the battery power demand smoother. The EMS decreases the battery power peaks and thus increases its life [16]. The splits of demanded power between battery and SC on the basis of SOC and vehicle movement state maximizes the use of SC during vehicle operation thereby reducing burden on the battery [17]. Adaptive FLC controls battery current on the basis of vehicle speed and driver command. The power split is done in parallel active topology of battery and SC [18]. The graded scheduling of ICE, battery and SC followed by updating rules minimizes battery aging cost and improves fuel efficiency of vehicle [19]. Higher output power and current is achieved by using battery-supercapacitor combination [20]. The battery and SC combination is used for keeping the bus voltage constant with load variation on dc bus. The scheme regulates dc bus voltage and limits the current for battery and SC both [21]. Improvement in size and efficiency affects the battery state of health (SoH). The EMS can control the power constraints of battery and SC thereby controlling the SoH of battery [22].

Pontryagin Minimum Principle (PMP) controllers are effective for instantaneous allocation of regenerative energy for two energy storage cases [23]. Pure Neural Network-based efficiency optimization may be used [24] but faster response with Fuzzy and Adaptive Fuzzy controllers for either battery or supercapacitor or both are extensively used for real-time control in conjunction with wavelet transform. However, assisted fuzzy controllers require offline training with previously recorded data set with real-time adjustment/tuning [25]. Deep Q-learning with Experience Replay has been tested with 2 identical Neural Network structures for power allocation for a hybrid battery thermal model for nurturing the SOC/SOH and efficiency of battery use [26].

The paper presents a control scheme for managing the power distribution between the battery and SC. The battery bank is followed by unidirectional buck-boost converter (UBBC) and SC followed by bidirectional buck-boost converter (BBBC). The overall HEV/EV system is nonlinear hence PID controller needs to be tuned very precisely. The parameters of PID controller is tuned by Teaching-Learning based optimization technique (TLBO), Particle swarm optimization technique (PSO) and Gray wolf optimization technique (GWO). The performance of controllers is evaluated by error based parameters, integral absolute error (IAE), integral squared error (ISE), integral of time weighted absolute error (ITAE) and integral of time weighted squared error (ITSE). The controller performance is checked for battery alone and battery-SC combination. The speed performance, battery voltage and super-capacitor voltage are analyzed for fixed speed and variable speed inputs. The section 2 of the paper gives details of modelling and circuit diagram of proposed scheme. Section 3 discusses proposed energy management scheme and tuning algorithm used. The result and discussion is given in section 4 and section 5 concludes the findings.

2. Modelling and Circuit Diagram

The supercapacitor (SC) is connected with the DC bus via a bidirectional buck-boost converter (BBBC) while the battery is connected through a unidirectional buck-boost converter (UBBC). The quick charge response makes it suitable for recharging through intermittent charging opportunities during regenerative braking. The reduced charge-discharge cycle increases the battery life.

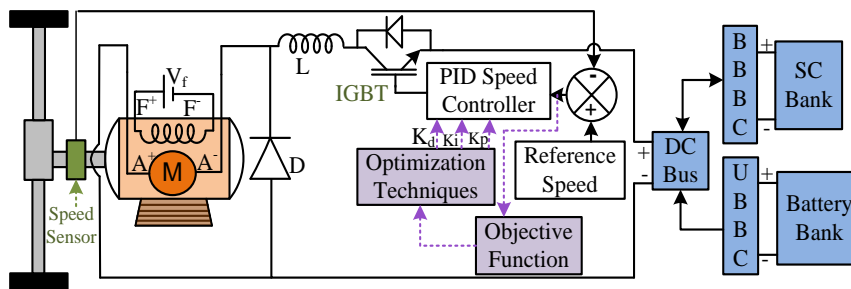


Fig. 1. Proposed structure of Energy distribution scheme

The proposed energy distribution scheme (EDS) is shown in fig (1). The power required is split between two available sources following energy conservation law. The demanded power is supplied by hybrid EDS of battery and super-capacitor and is mentioned in equation (1)

$$P_{load} = P_{battery} + P_{SC} \tag{1}$$

Where P_{load} is the power required by the load, P_{SC} and $P_{battery}$ are power supplied by super-capacitor and battery respectively. In most cases, Battery is used for supplying base load whereas SC is deployed for peak load. The battery burden from charge-discharge would cycle would be released if the kinetic energy generated during regeneration is absorbed by the SC. The kinetic energy (E_{ke}) is given in equation (2).

$$E_{ke} = \frac{1}{2}mv^2 \tag{2}$$

Where m is the mass of the vehicle, v is the speed. As per the equation of motion (equation 3)

$$v = v_0 + at \tag{3}$$

v_0 is the initial speed, a is acceleration and t is time. The kinetic energy is equation (4)

$$E_{ke} = \frac{1}{2}m(v_0 + at)^2 \tag{4}$$

The first derivative gives the power delivered by SC for absorbing the entire kinetic energy of the vehicle as in equation (5)

$$\frac{dE_{ke}}{dt} = P_{SC} = m.a.v_0 + m.a^2.t \tag{5}$$

In the proposed EMS the PID controller controls the switching MOSFET for dc bus voltage control.

2.1. Modeling of DC Motor

The motor needed for the purpose should be capable of operating all quadrants as motoring and regenerating both modes would be required during operation. DC motors are capable of operating in such conditions. The power delivered (P_m) during both the modes is known by equation (6)

$$P_m = \frac{T_m \cdot N_m}{9550\eta_m} \tag{6}$$

T_m is motortorque, N_m is motor speed and η_m is motor efficiency. The EMF equation of the motor is mentioned in equation (7)

$$u = E + R.I + L.\frac{dI}{dt} + \delta(i) \tag{7}$$

Where u is terminal voltage, E is induced emf, I is current, L is armature inductance (i) represents the armature reaction drop. The torque of the motor is determined by the energy conversion principle [27] from equation (8)

$$\lambda\omega = (E - \delta).I \tag{8}$$

λ is the motor torque and ω is angular speed.

2.2. Modeling of Battery

The battery model is represented in fig. (2) as

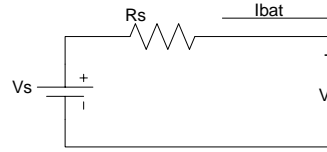


Fig. 2. Battery Model

The voltage and power are determined by equations (9-10)

$$V_s = I_{bat} \cdot R_s + V_t \quad (9)$$

$$P_{bat} = V_s \cdot I_{bat} - I_{bat}^2 \cdot R_s \quad (10)$$

I_{bat} is current drawn from the battery, V_s is sources voltage, R_s is the source resistance. The current drawn from the battery is determined by equation (11)

$$I_{bat} = \frac{V_s - \sqrt{V_s^2 - 4 \cdot R_s \cdot P_{bat}}}{2 \cdot R_s} \quad (11)$$

Change of battery SOC (Δ SoC) is known through equation (12)

$$d(\text{SoC}) = \frac{I_{bat} \cdot dt \cdot \eta_{bat}}{Q_{bat}} \quad (12)$$

dt is the change of time, η_{bat} battery efficiency and Q_{bat} is charged in the battery.

2.3. Modeling of Supercapacitor

In supercapacitors, the electrical energy is mainly stored through the establishment of the double-layer capacitor structure at the interface between the electrolyte and the electrodes. The Electrostatic Charge Transfer (ECT) characteristic outcome n a high degree of recyclability [29]. SCs offer high capacitance as compared to traditional or ordinary capacitors because of the electrode's high specific area. Electrode specific mainly depends upon the materials used and their physical properties. SC gives high power density, fast charging & discharging, and an almost unlimited life time. In large power fluctuations and or vehicle starting time, SC can be discharged or charged in such a way that relieves the stress on the battery. The capacitance of the supercapacitor (SOC_{SC}) can be achieved by equation (13)

$$SOC_{SC} = \frac{C \cdot (V - V_{mn})}{C \cdot (V_{mx} - V_{mn})} = \frac{(V - V_{mn})}{(V_{mx} - V_{mn})} \quad (13)$$

Where V_{mx} and V_{mn} are maximum and minimum permissible voltage for supercapacitor and C is the capacitance.

2.4. Circuit Description of Unidirectional Buck-Boost Converter

The unidirectional buck-boost converter is used for obtaining the terminal voltage above and below the input voltage as per the duty cycle (D) and is used for single-direction operation. The duty cycle is determined by equation (14)

$$D = \frac{T_{on}}{T_{on} + T_{off}} = \frac{T_{on}}{T_s} \quad (14)$$

Where T_{on} is ON time, T_{off} is OFF time and T_s is the total time for MOSFET respectively.

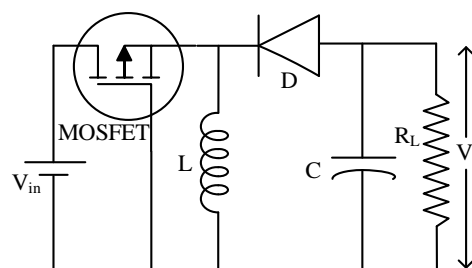


Fig. 3. Circuit model of UBBC

Fig. (3) represents the circuit model of UBBC. In mode I operate the controlling MOSFET fires which make the switch shorted and diode reverse biased. The effective figure becomes as in fig. 4 (a).and Voltage stored across the inductor (V_{L1}) is given in equation (15)

$$V_{L1} = V_{in} \cdot D \cdot T_s \tag{15}$$

D is the duty cycle, during mode II the controlling MOSFET commutates and behaves as an open switch, the resulting figure becomes as in fig. 4(b). The inductor voltage (V_{L2}) is known from equation (16)

$$V_{L2} = V_o \cdot (1 - D) \cdot T_s \tag{16}$$

Since Inductor Voltage (V_L) as given in equation (17) is

$$V_L = V_{L1} + V_{L2} \tag{17}$$

Due to zero volt second production in inductor, output voltage (V_o) can be known from equation (18)

$$V_o = -V_{in} \frac{D}{1 - D} \tag{18}$$

The unidirectional converter output depends on and off period of the controlling element [30].

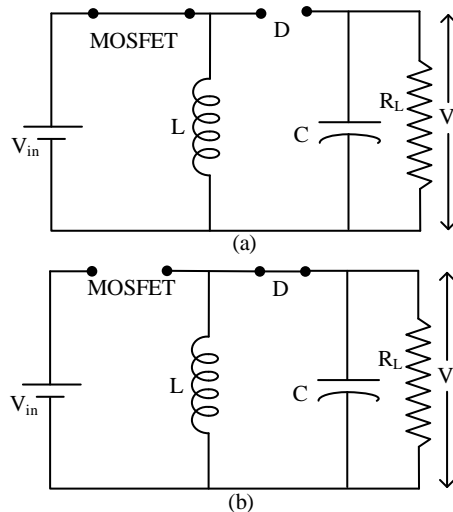


Fig. 4 (a) (b). Operation mode of UBBC converter

2.5. Circuit Description of Bidirectional Buck-Boost Converter

The charging and discharging operations of the battery and supercapacitor required a bidirectional buck-boost converter. It reduces the size, cost, and complexity of the control circuit.

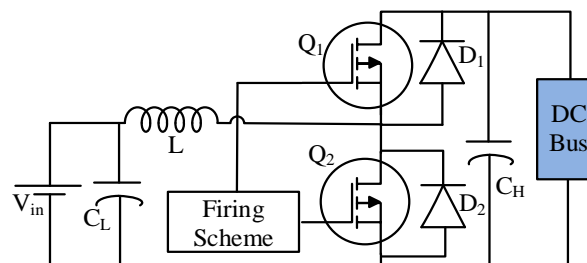


Fig. 5. Circuit Model of BBBC

In the circuit shown in fig. 5, The modulation of Q_2 with diode D_1 provides a boost mode of operation while modulation of Q_1 provides the buck mode. The converter operates in a steady state is obtained by designing switching of Q_1 and Q_2 [31].

In mode 1 operation Q_1 is off, Q_2 is on and diode D_1 and D_2 are reverse biased (Fig. 6a). The working is in boost mode, inductor charges and current through it increases. The circuit equations are mentioned in (19-20).

$$L \frac{di_1}{dt} = V_2 \tag{19}$$

$$\frac{di_a}{dt} = \frac{V_1}{L} - \frac{E_b}{L} - \frac{r_a}{L} i_a \tag{20}$$

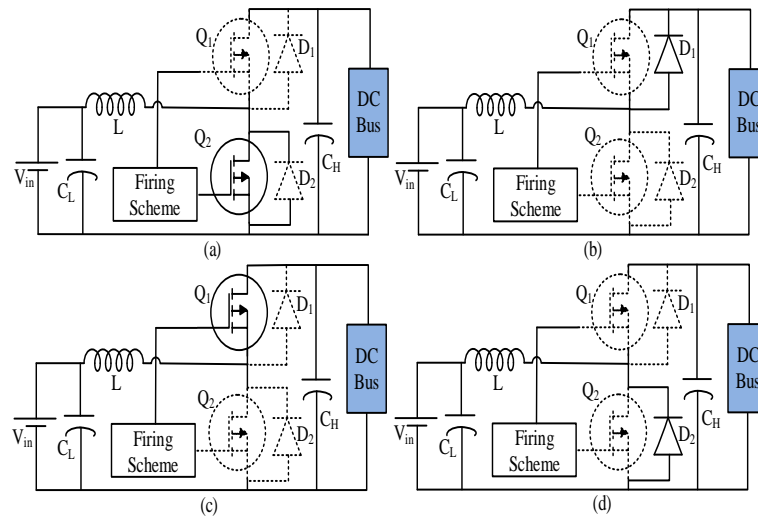


Fig. 6. Operation mode of BBBC converter

In mode 2, both the MOSFETS are commutates, and the diode D1 conducts (fig. 6b). The output voltage of the converter is fed across the motor. The boost mode increases the battery voltage. The circuit equations are mentioned in (21-22).

$$\frac{dV_1}{dt} = \frac{i_a}{C_h} \tag{21}$$

$$\frac{dV_2}{dt} = \frac{V_b}{R_b C_1} - \frac{V_2}{R_b C_1} - \frac{i_1}{C_1} \tag{22}$$

In mode 3, Q1 is ON while Q2 is OFF, Both the diodes being reverse biased (fig. 6c). Buck mode of operation is achieved. The circuit equations are mentioned in (23-24).

$$\frac{di_1}{dt} = \frac{-V_1}{L} + \frac{V_2}{L} \tag{23}$$

$$\frac{dV_2}{dt} = \frac{V_b}{R_b C_1} - \frac{V_2}{R_b C_1} - \frac{i_1}{C_1} \tag{24}$$

In mode 4, Both the MOSFETS are turned off and D2 conducts (fig. 6d). The circuit equations are mentioned in (25-26).

$$\frac{dV_1}{dt} = \frac{i_1}{C_h} - \frac{i_a}{C_h} \tag{25}$$

$$\frac{di_a}{dt} = \frac{V_1}{L} - \frac{E_b}{L} - \frac{r_a}{L} i_a \tag{26}$$

V_1 is battery side voltage, V_2 is the output voltage, L is inductance, i_a is current, E_b is battery emf, C_1 is shunt capacitance across the battery, C_h is shunt capacitance across dc bus and r_a is resistance. The converter is suitable for driving the motor as well as the regenerative action.

3. Proposed Energy Management Schemes

Tuning of controller is most important aspect of controller design [32]. The error signal ($e(t)$) is the difference of reference speed (ω_{ref}) and actual speed (ω_r). The PID equations are based on the error signal. The error signal is determined by equation (27) and the controller action equation is given in equation (28)

$$e(t) = \omega_{ref} - \omega_r \quad (27)$$

$$u(t) = K_p \cdot e(t) + K_i \int_0^t e(t) dt + K_d \frac{de(t)}{dt} \quad (28)$$

Where $u(t)$ is the control signal, K_p , K_i and K_d are the proportional, Integral, and differential gain respectively. For determining suitable control parameters, several integral performance criteria are developed. These criteria are based on the error signal produced. The integral absolute error (IAE) integrated absolute error without adding weight to it and is given in equation (29).

$$IAE = \int_0^{\infty} |e(t)| dt \quad (29)$$

The integral squared error (ISE) integrates the square of the error penalizing a larger error as compared to a smaller one. The ISE equation is given in equation (30).

$$ISE = \int_0^{\infty} \{e(t)\}^2 dt \quad (30)$$

The integral of the time-weighted absolute of the error (ITAE) integrates the error multiplied with time. The criteria future error harder than the error that occurred at starting and is given in equation (31)

$$ITAE = \int_0^{\infty} t \cdot |e(t)| dt \quad (31)$$

The integral of time-weighted squared error (ITSE) minimizes the large initial error effect by integrating the square of the error multiplied with time. The ITSE equation is given in equation (32).

$$ITSE = \int_0^{\infty} t \cdot \{e(t)\}^2 dt \quad (32)$$

The objective function (obj) for the optimization is to minimize the error. The objective function is given in equation (33)

$$Obj = \text{Min}[e(t)] \quad (33)$$

The designed Simulink model implements TLBO, PSO, and GWO optimization techniques. The initial values of the parameters are declared before initializing the optimization process. The stopping criteria for the optimization process are the smallest value of the error.

3.1 Gain Tuning by TLBO Technique

TLBO is a population-based technique. To ensure the global solution, it uses a population of solutions. The basis of the TLBO method is influenced by the teaching-learning process in the classrooms. The grades/results are assumed as the output. In general, a Well-educated individual who shares his or her information and experience with the learners is called a teacher. A set of learners is known as population [33]. The algorithm is classified majorly into two segments.

3.1.1 Teacher Phase

In the teacher phase, the student learns from the teacher. The highly qualified learned, and knowledgeable person is reckoned as a teacher. The teachers put effort into a student for improving their knowledge and scoring better marks or grades. For using this concept in optimization, the best student is selected as "Teacher". If T^n is a teacher (most feasible solution) at n th teaching-learning (T-L) cycle and T_i^n is the i th parameter of the teacher at n th T-L cycle. The deviation of teacher and mean result in the i th subject is mentioned in equation (34).

$$D_i^n = r \cdot (T_i^n - T_f M_i^n) \quad (34)$$

Where M_i^n mean result of learners in an i th subject, T_f is teaching factor which decided the value by which mean is to be changed. It should be either 1 or 2. 'r' is a random scalar varying between 0 to 1. The performance of a student (feasible solution) is improved by shifting their position towards the teacher as mentioned in equation (35).

$$T_{new_i}^n = T_{old_i}^n + D_i^n \quad (35)$$

If a new solution is better than the old one, it is accepted otherwise it is rejected.

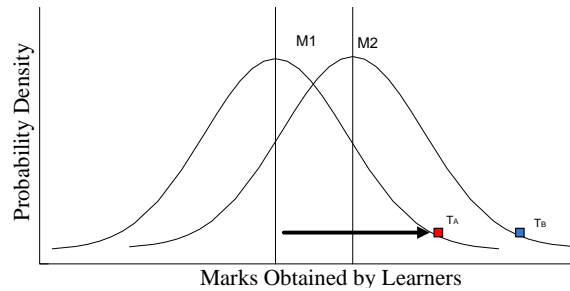


Fig. 7. Students/Learners marks obtained distribution taught by two different teachers.

If two teachers namely Tr1 and Tr2 are teaching the same course with content to similar quality learners in two separate sections. Fig.(7) illustrates the obtained marks distribution of the students/learners of the two separate sections assessed by the teachers Tr1 & Tr2. Curve-1 corresponds to the Tr1 and their section [34]. The Normal Distribution (ND) is anticipated for obtained grades, but practically it may have skew components. The ND is defined as $f(x)$ which is given in equation (36)

$$f(x) = \frac{1}{\sigma} \sqrt{2\pi} e^{-\frac{(x-\mu)^2}{2\sigma^2}} \quad (36)$$

Where σ =Variance, μ =Mean, and x =any random value requiring NS.

From Fig. (7) It is observed that curve-2 shows superior results as compared to curve-1 and thus it may be concluded that Tr2 is better than Tr1 in terms of training. The key difference in the two results or marks distribution lies in their mean where M2 (Curve-2 mean) is greater than M1 (Curve-1 mean). Thus, a good trainer produces superior mean results or better learning outcomes.

In this Student phase, the knowledge of the student (feasible solution) is enhanced by mutual interaction. If the learning of a student is increased the less learned student moves towards it. The random possible solutions (S_a^n) and (S_b^n) are chosen where a and b are random numbers ($a \neq b$) and $(a,b) \in [1,N]$. The fitness value is determined by a fitness function $F(s)$ in equation (37-38) as

If $F(S_a^n) > F(S_b^n)$

$$S_{new_ai}^n = S_{ai}^n + r * (S_{ai}^n - S_{bi}^n) \quad (37)$$

Otherwise

$$S_{new_ai}^n = S_{ai}^n - r * (S_{ai}^n - S_{bi}^n) \quad (38)$$

Where $S_{new_ai}^n$ is the i th variable of new feasible solution in the student phase. The fitness function is evaluated in equation (39) as

$$S_{new_a}^n = S_{new_sp_a}^n \quad (39)$$

Otherwise $S_{new_a}^n$ unchanged

If $F(S_{new_sp_a}^n) > F(S_{new_a}^n)$

The simulation parameters used for TLBO optimization in this paper are given in table (1)

Table 1. TLBO Parameters	
Size	Count
Generation	10
Population	10

3.2 Gain Tuning by Particle Swarm Optimization

Particle Swarm Optimization was given by Kennedy and Eberhart in 1995. The search-based heuristic algorithm of swarms like birds, fishes and other natural species [35]. In the algorithm, the population of particles is randomly initialized with an initial velocity and position. The velocity and position are updated by improving the fitness value. Then the swarm of these particles is directed towards the optimal position for having the optimal solution. The velocity and position of the particle are given in equation (40-41):

$$V_{(k+1)} = wV_{(k)} + c_1r_1(pBest(k) - x(k)) + c_2r_2(gBest(k) - x(k)) \quad (40)$$

$$x_{(k+1)} = x_{(k)} + V_{(k+1)} \quad (41)$$

Where $V_{(k+1)}$ is new velocity, $x_{(k+1)}$ is a new position, $V_{(k)}$ is old velocity, $x_{(k)}$ is old position, $gBest$ global best in the population, w is an inertial coefficient, $C1$ and $C2$ are cognition and social learning rates respectively, $r1$ and $r2$ are random scalars. Since it does not use the gradient of the objective function, it is also suitable for nonlinear and time-variant functions [36]. The simulation parameters used for PSO optimization in this paper are mentioned in table (2).

Table 2. PSO Parameters

Parameter	Value
Swarm Population	10
Minimum Inertia coefficient	0.98
Maximum Inertia coefficient	1
Social coefficient, C1	2
Cognitive coefficient, C1	2

3.3 Gain Tuning by Gray-Wolf Optimization

Gray-wolf optimization (GWO) is a unique type of algorithm under the category of swarm intelligence. It is based on the hunting mechanism and the hierarchical leadership of gray wolves. α s are the most dominating ones. The β s are placed next to α and usually known as the subordinate or advisor wolves and they assist α in taking decisions and controlling group movement. The third category in the hierarchy of dominance is δ wolves which are following the higher-level wolves only dominating the ω wolves. The last category in the hierarchy is ω wolves. The gray wolves hunting modeling is as follows; 1) Social-hierarchy, chasing and following the target; 2) Pursuing, enclosing, and irritating the target till it stops moving; 3) the targeted attack [37].

3.1.1 Social Hierarchy Phase

The hierarchical structure suggests that the best solution among the available should be assigned to alpha (α), followed by subsequent solutions are assigned to beta (β) and delta (δ). Finally, the balance solutions should be assigned to omega (ω).

3.1.2 Target Enclosing Phase

The enclosing of the target is done by the gray wolves in this phase of hunting. The mathematical model for this can be given in equation (42-45) as:

$$Y = |KX_p(t) - X(t)| \quad (42)$$

$$X(t+1) = X_p(t) - AY \quad (43)$$

$$A = a.(2r_1 - 1) \quad (44)$$

$$K = 2.r_1 \quad (45)$$

Where t is the total iteration, the target location is represented by Y . X_p and X represents the gray wolf's position. A and K are the coefficient vectors. During the iteration, the value of a decreases linearly from 2 upto 0 and r_1 and r_2 are randomly chosen for the interval $[0, 1]$.

3.1.3 Hunting Phase

From the above discussion, it is clear that α , β , and δ are the best solutions set for obtaining the global optima. Thus, the first three sets of best-accomplished solutions to this point are recorded and facilitated to other searching agents, including ω , to appraise the current positions as per the position of the best search agent. The equations (46-48) are utilized for this purpose.

$$D_\alpha = K_1 X_\alpha - X, D_\beta = K_2 X_\beta - X, D_\delta = K_3 X_\delta - X \quad (46)$$

$$X_1 = X_\alpha - A_1 Y_\alpha, X_2 = X_\beta - A_2 Y_\beta, X_3 = X_\delta - A_3 Y_\delta \quad (47)$$

$$X_{new} = (X_1 + X_2 + X_3) / 3 \quad (48)$$

where X is the position of ω wolves, X_α , X_β , X_δ are the position of α , β , δ wolves, D_α , D_β , D_δ are the distance between α , β , δ with ω respectively.

3.1.4 Target Attacking Phase

To find the mathematical model of the target attacking phase, the linear decrease of 'a' (from 2 to 0) causes a decrease in the A range. Therefore A is a random number ranging between $[-a, a]$. When random values of A are between $[-1, 1]$, the next hunting agent location is positioned between the current spot and target spot. The $A < 1$ shows the condition

where the target is confronted by the wolves . The simulation parameters used for GWO optimization in this paper are given in Table (3).

Table 3. GWO Parameters

Parameter	Value
Population Size	10
Generation Size	10
Dimension	2

4. Results and Discussions

For evaluating the performance of the proposed strategy and optimization techniques, simulation work is carried out in MATLAB/Simulink. The gain of PID controller (K_p , K_i , K_d) is determined by Ziegler Nichlos (ZN Method for reference). The design parameters used for simulation are summarized in table (4).

Table 4. Simulation parameters

Design Parameter	Value
Bus Voltage	240 V
Driving motor	DC, separately excited
Power rating	5 HP
Operating Voltage	240 V
Speed rating	1750 rpm
Field Voltage	150 V

The optimized gains of the PID controller along with Z-N gains are given in table (5).

Table 5. Tuned value of controller gains

Optimization Method	K_p	K_i	K_d
ZN	0.001	0.02	0.0001
TLBO	1.6992	1.1802	0.0958
PSO	19.9423	11.8608	0.8979
GWO	20	16.1832	1.1338

4.1 Battery Powered Drives

In the first section of the simulation, the drive is run by battery only for both the base and peak load. The gains of PID controllers are optimized by the mentioned methods. The performance is evaluated for fixed and variable speed as a reference. The obtained speed result is compared with the input reference speed

4.1.1. Performance of Battery-Powered Drives by Applying Fixed Reference Speed

In this performance analysis, a fixed speed of 500 rpm is provided as input. The drive speed profile with the battery alone is given in Fig. (8). A comparison of obtained speed with reference speed with differing gains is indicated.

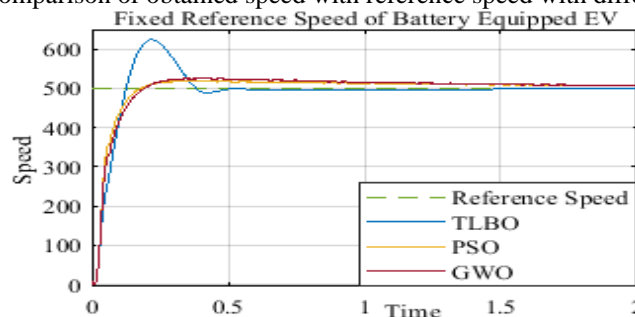


Fig. 8. Speed profile for battery alone system with a fixed reference

4.1.2. Performance of Battery-Powered Drives by Applying Variable Reference Speed

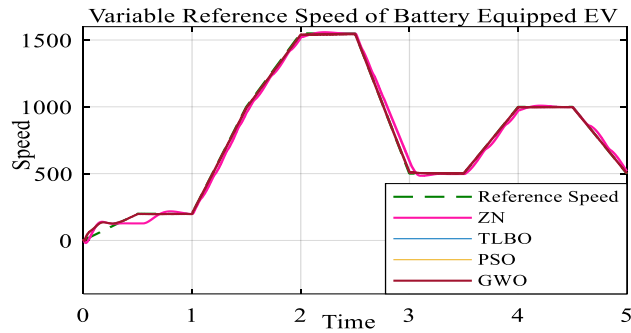


Fig. 9. Speed profile for battery alone system with variable reference

In this simulation, a variable drive cycle is fed as reference speed. The speed profile obtained by the tuned parameters of the PID controller for the demanded power is shown in Fig.(9).An analysis of results obtained in fig. (8)and (9) shows that gain parameters optimized by the GWO algorithm provided a better speed profile.

4.2 Supercapacitor and Battery-Powered Drives

In this mode,thesupercapacitor and battery aresimultaneously connected to the dc bus through BBBC and UBBC respectively. The speed and voltage profilesareanalyzed for different PID gains tuned by various optimization algorithms and the conventional Z-N method.

4.2.1 Performance of Supercapacitor and Battery-Powered Drives by Applying Fixed Reference Speed

Fig (10a) shows the speed variation for supercapacitor and battery-fed drives. The results for different gains obtained from the three implemented cFixed Reference Speed of Battery and Supercapacitor Equipped EV

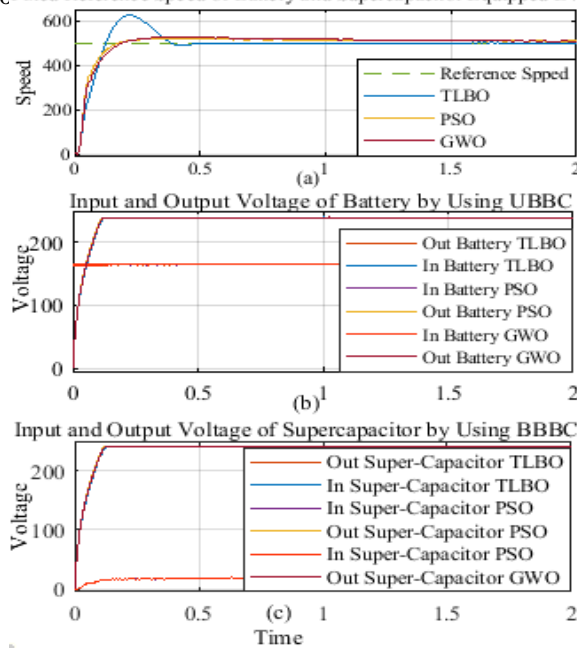


Fig. 10. Speed and Voltage profile for battery-SC combination system with the fixed reference

The voltage profile indicated in fig. (10b-10c) indicates a smooth voltage stabilization for dc Bus for both the UBBC and BBBC converters.

4.2.2 Performance of Supercapacitor and Battery-Powered Drives by Applying Variable Reference Speed

The speed profile for different gain parameters of PID controller tuned by ZN, TLBO, PSO, and GWO method is shown in fig (11). The result compared with the reference speed shows the supremacy of the GWO algorithm in all implemented schemes.

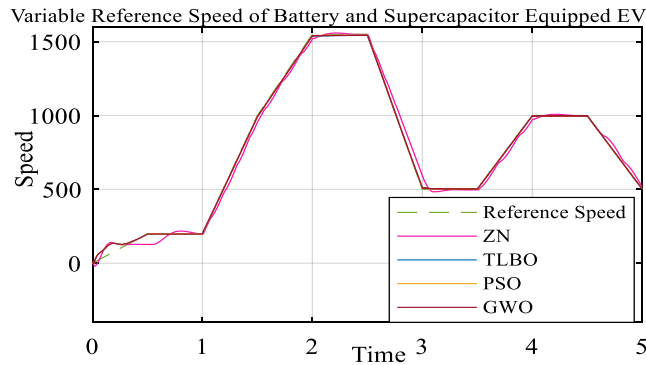


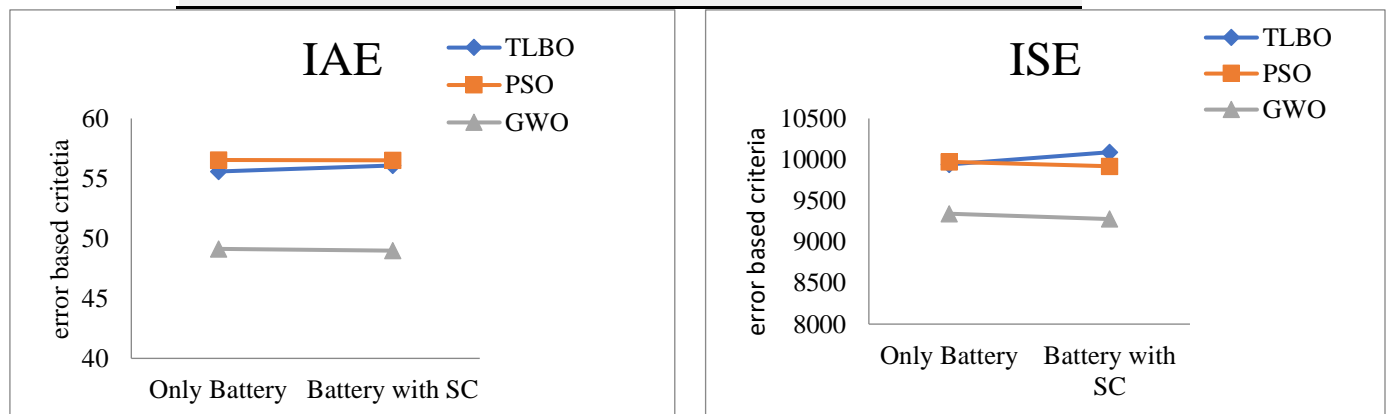
Fig. 11. Speed profile for battery-SC combination system with variable reference

4.3 Performance Parameters Values

The values of performance criteria are the indicator of the performance of the controller. The value of IAE is 55.58, 56.54, 49.13 for TLBO, PSO, GWO optimization techniques respectively when only battery is connected and the respective value for battery-SC hybrid input was 56.08, 56.51, 49.13. The lowest value is observed as 48.98 for battery-SC input with GWO optimization. The ISE parameter for TLBO, PSO, and GWO are 9941, 9973, 9342 for the battery alone and 10090, 9919, 9277 for battery-SC input, The results of ISE again indicate the lowest value for battery-SC combination with GWO technique. The value of ITAE for the three techniques are 26.01, 26.17, 22.17 for the battery alone and 26.09, 26.17, 22.06 indicating the lowest for battery-SC combination tuned by GWO techniques. The fourth parameter, ITSE, is observed as 583.5, 602.4, 450.5 for the battery alone and 594.9, 601.6, 447.1, showing the lowest value of battery-SC combination tuned by GWO technique. The observed value of performance criteria is summarized in table (6) and the comparison of performance parameter values is given in fig. (12).

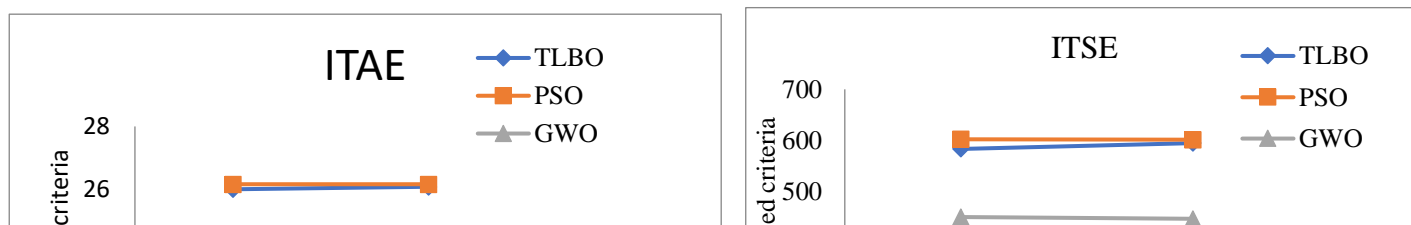
Table 6. Value of performance parameters

Power Source	Technique	IAE	ISE	ITAE	ITSE
Battery alone	TLBO	55.58	9941	26.01	583.5
Battery alone	PSO	56.54	9973	26.17	602.4
Battery alone	GWO	49.13	9342	22.17	450.5
Battery and SC	TLBO	56.08	10090	26.09	594.9
Battery and SC	PSO	56.51	9919	26.17	601.6
Battery and SC	GWO	48.98	9277	22.06	447.1



(a) IAE

(b) ISE



criteria

ed criteria

(c) ITAE

(d) ITSE

Fig 12: Value of Performance criteria for different optimization algorithms

The result comparison shown in fig (12 a-d) shows that IAE, ISE, and ITAE value is minimum when gain parameters are optimized by the GWO algorithm.

5. Conclusion

The paper presented the battery and supercapacitor fed drives controlled by the PID controller. The gain of the PID controller is tuned by three meta-heuristic search algorithms namely TLBO, PSO, and GWO. A simulation scheme was designed in MATLAB/Simulink for carrying out the study. The performance of the controller is evaluated by performance criteria IAE, ISE, ITAE, and ITSE. The speed profile for controller gains was compared for the implemented optimization techniques along with the conventional Z-N method. The value of performance parameters IAE, ISE, TAE and ITSE is obtained as 48.98, 9277, 22.06 and 447.1 for the GWO algorithm with hybrid input, which is the lowest among all implemented methods. The result shows the supremacy of the GWO method. Further, the result of the battery alone and hybrid input was compared. The simulation result indicates that the combination of battery and supercapacitor provides a better result as compared with the battery-alone system. The speed and voltage profiles are also satisfactory.

References

- [1]. M. Khattak, A. Omran, H. Andjani, N. Mardhiah and S. Kazi, "Accretion of Indonesia's Energy Sector Through Renewable Energy", *Journal of Engineering Science and Technology*, Vol. 14, No. 6, pp. 3628-3641, 2019.
- [2]. Q. Imran, R. Amranand, Z. Khalid, "Energy crisis, greenhouse gas emissions and sectoral growth reforms: repairing the fabricated mosaic", *Journal of Cleaner Production*, Vol. 112, no. 5, pp. 3657-3666, 2016.
- [3]. P. Balasubramanian and P. Karthickumar, "Indian energy crisis - A sustainable solution", *IEEE-International Conference on Advances in Engineering, Science and Management (ICAESM -2012)*, pp. 411-415, 2012.
- [4]. L. Tripathi, A.K. Mishra, A.K. Dubey, C.B. Tripathi and P. Baredar, "Renewable energy: An overview on its contribution in current energy scenario of India", *Renewable and Sustainable Energy Reviews*, Vol. 60, pp. 226-233, 2016.
- [5]. G. Jacob, D. Passigli, H. Henderson, J. Ramanathan, "Catalytic Strategies for Socially Transformative Leadership: Leadership Principles, Strategies and Examples", *Cadmus*, Vol 4, no. 2, pp. 06-45, 2020.
- [6]. J. Rissman, C. Bataille, E. Masanet, N. Aden, W.R. Morrow, N. Zhou, N. Elliott et al., "Technologies and policies to decarbonize global industry: Review and assessment of mitigation drivers through 2070", *Applied Energy*, Vol. 266, p. 114848, 2020.
- [7]. Y. Cheng, V. M. Joeri and P. Lataire, "Research and test platform for hybrid electric vehicle with the super capacitor based energy storage," *European Conference on Power Electronics and Applications*, pp. 1-10, 2007.
- [8]. X. Lu, Y. Wu, J. Lian, Y. Zhang, C. Chen, P. Wang and L. Meng, "Energy management of hybrid electric vehicles: A review of energy optimization of fuel cell hybrid power system based on genetic algorithm", *Energy Conversion and Management*, Vol. 205, p. 112474, 2020.
- [9]. V. I. Herrera, H. Gaztañaga, A. Milo, A. Saez-de-Ibarra, I. E. Otadui and T. Nieva, "Optimal energy management of a battery-supercapacitor based light rail vehicle using genetic algorithms", *IEEE Energy Conversion Congress and Exposition (ECCE 2015)*, pp. 1359-1366, 2015.

- [10]. V. Herrera, A. Milo, H. Gaztañaga, I. E. Otadui, I. Villarreal and H. Camblong, “Adaptive energy management strategy and optimal sizing applied on a battery-supercapacitor based tramway”, *Applied Energy*, Vol.169, pp. 831-845, 2016.
- [11]. S. Hussain, M.U. Ali, G.-S. Park, S.H. Nengroo, M.A. Khan and H.-J. Kim, “A Real-Time Bi-Adaptive Controller-Based Energy Management System for Battery–Supercapacitor Hybrid Electric Vehicles”, *Energies*, Vol.12, pp. 4662, 2019.
- [12]. V. A. Shah, S. G. Karndhar, R. Maheshwari, P. Kundu and H. Desai, "An energy management system for a battery ultracapacitor Hybrid Electric Vehicle", *International Conference on Industrial and Information Systems (ICIIS)*, pp. 408-413, 2009.
- [13]. A. Castaings, W. Lhomme, R. Trigui and A. Bouscayrol, "Comparison of energy management strategies of a battery/supercapacitors system for electric vehicle under real-time constraints", *Applied Energy*, Vol. 163, pp. 190-200, 2016.
- [14]. Q. Zhang, L. Wang, G. Li and Y. Liu, “A real-time energy management control strategy for battery and supercapacitor hybrid energy storage systems of pure electric vehicles”, *Journal of Energy Storage*, Vol. 31, pp. 1-9, 2020.
- [15]. J. Hu, D. Liu, C. Du, F. Yan and C. Lv, “Intelligent energy management strategy of hybrid energy storage system for electric vehicle based on driving pattern recognition”, *Energy*, Vol. 198, p.117298, 2020.
- [16]. F. Akar, Y. Tavlasoglu and B. Vural, "An Energy Management Strategy for a Concept Battery/Ultracapacitor Electric Vehicle with Improved Battery Life", *IEEE Transactions on Transportation Electrification*, Vol. 3, no. 1, pp. 191-200, 2017.
- [17]. Azizi, I., Radjeai, H., “A new strategy for battery and supercapacitor energy management for an urban electric vehicle”, *Electrical Engineering*, Vol.100, pp. 667–676, 2018.
- [18]. H. Yin, W. Zhou, M. Li, C. Ma and C. Zhao, "An Adaptive Fuzzy Logic-Based Energy Management Strategy on Battery/Ultracapacitor Hybrid Electric Vehicles", *IEEE Transactions on Transportation Electrification*, Vol. 2, no. 3, pp. 300-311, 2016.
- [19]. Li, Shuangqi & Gu, Chenghong & Zhao, Pengfei & Cheng, Shuang. (2021) “Adaptive Energy Management for Hybrid Power System Considering Fuel Economy and Battery Longevity”, *Energy Conversion and Management*. Vol. 235, p.114004, 2021.
- [20]. J. Norbakyah and A. Salisa, “Effectiveness of Battery-Ultracapacitor Combination for Energy System Storage in Plug-In Hybrid Electric Recreational Boat (PHERB)”, *Journal of Engineering Science and Technology*, Vol. 14, No. 1, pp. 108-121, 2019.
- [21]. N. R. Tummuru, M. K. Mishra and S. Srinivas, "Dynamic Energy Management of Hybrid Energy Storage System With High-Gain PV Converter", *IEEE Transactions on Energy Conversion*, vol. 30, no. 1, pp. 150-160, 2015.
- [22]. N. Rizoug, T. Mesbahi and R. Sadoun, “Development of new improved energy management strategies for electric vehicle battery/supercapacitor hybrid energy storage system”, *Energy Efficiency*, Vol 11, pp. 823–843, 2018.
- [23]. C. Zheng, W. Li and Q. Liang, "An Energy Management Strategy of Hybrid Energy Storage Systems for Electric Vehicle Applications", *IEEE Transactions on Sustainable Energy*, Vol. 9, no. 4, pp. 1880-1888, 2018.
- [24]. J. Moreno, M. E. Ortuzar and J. W. Dixon, "Energy-management system for a hybrid electric vehicle, using ultracapacitors and neural networks", *IEEE Transactions on Industrial Electronics*, vol. 53, no. 2, pp. 614-623, 2006.
- [25]. C. Gao, J. Zhao, J. Wu and X. Hao, "Optimal fuzzy logic based energy management strategy of battery/supercapacitor hybrid energy storage system for electric vehicles", *12th World Congress on Intelligent Control and Automation (WCICA)*, pp. 98-102, 2016.
- [26]. W. Li, H. Cui, T. Nemeth, J. Jansen, C. Ünlübayir, Z. Wei, L. Zhang, Z. Wang, J. Ruan, H. Dai, X. Wei and D. U. Sauer, “Deep reinforcement learning-based energy management of hybrid battery systems in electric vehicles”, *Journal of Energy Storage*, Vol. 36, p. 102355, 2021.
- [27]. N. K. Sinha, C. D. Dicenzo and B. Szabados, "Modeling of DC Motors for Control Applications", *IEEE Transactions on Industrial Electronics and Control Instrumentation*, Vol. 21, no. 2, pp. 84-88, 1974.
- [28]. J. Peng, H. Fan, H. He and D. Pan, “A Rule-Based Energy Management Strategy for a Plug-in Hybrid School Bus Based on a Controller Area Network Bus”, *Energies*, Vol. 8, pp. 5122–5142, 2015.
- [29]. L. Zhang, X. Hu, Z. Wang, F. Sun and D. G. Dorrell, “A review of supercapacitor modeling, estimation, and applications: A control/management perspective”, *Renewable and Sustainable Energy Reviews*, Vol. 81, Part 2, pp. 1868-1878, 2018.
- [30]. M. H. Rashid, “DC-DC Converters” in *Power Electronics Handbook*, 3rd ed., California, U.S. State, Academic Press, 2011, Ch. 13, pp. 251-255.
- [31]. P. Pany, R.K. Singh and R. K. Tripathi, “Bidirectional DC-DC converter fed drive for electric vehicle system”, *International Journal of Science and Technology*, Vol.3, no. 3, pp. 101-110, 2011.

- [32]. V. Bhat, I. Thirunavukkarasu and S. Priya, “Design of Centralized Robust Pi Controller for a Multivariable Process”, *Journal of Engineering Science and Technology*, Vol. 13, No. 5, pp. 1253-1273, 2018.
- [33]. H. S. Gill, B. S.Khehra, A. Singh and L. Kaur, “Teaching-learning-based optimization algorithm to minimize cross entropy for Selecting multilevel threshold values”, *Egyptian Informatics Journal*, Vol. 20, Issue 1, pp. 11-25, 2019.
- [34]. R.V. Rao, V.J. Savsani and D.P. Vakharia, “Teaching-learning-based optimization: A novel method for constrained mechanical design optimization problems”, *Computer-Aided Design*, Vol. 43, Issue 3, pp. 303-315, 2011.
- [35]. J. Kennedy and R.Eberhart, “Particle Swarm Optimization”, *Proc. IEEE Conference*, vol 4, pp. 1942-1948, 1995.
- [36]. X. S. Yang, “Particle Swarm Optimization”, in *Nature-Inspired Optimization Algorithms*, 1sted., London, UK, Elsevier 2014, Ch. 07, pp 99-103.
- [37]. W. Xin, "Photovoltaic Power Prediction Based on RBF Neural Network Optimized by Gray Wolf Algorithm", *3rd International Conference on Control and Robots (ICCR)*, pp. 226-230, 2020.

Nomenclatures	
P_{load}	power required by the load
P_{sc}	power supplied by super-capacitor
$P_{battery}$	power supplied by Battery
M	Mass of vehicle
V	Velocity
T_m	Torque of the motor
N_m	Motor Speed
I_b	Current drawn from the battery
V_{oc}	Open circuit voltage
R_{in}	Internal Resistance of battery
SOC	State of charge
J_m	Energy Consumption of Battery
SOC_{sc}	State of charge for Supercapacitor
D	Duty Cycle
V_{in}	Input Voltage
V_o	Output Voltage
L	Inductance
K_p	Proportional gain
K_i	Integral gain
K_d	Differential gain
IAE	Integrated absolute error
ISE	Integral squared error
$ITAE$	Integral of the time-weighted absolute of the error
$IISE$	Integral of time-weighted squared error
T	Teacher
S	Student
M	Mean Result
R	Random scalar
X	Position
K	Coefficient factor
Greek Symbols	
Σ	Variance
μ	Mean
α, β, γ	Hierarchy of wolf
Abbreviations	
TLBO	Teacher Learning Based Optimization
PSO	Particle Swarm Optimization
GWO	Grey Wolf Optimization
UBBC	Unidirectional Back to Back Converter
BBBC	Bi-directional Back to Back Converter